

Date 2013
Author Jong, P. de, M.R. Renilson and F. van Walree

Address Delft University of Technology
Ship Hydromechanics and Structures Laboratory
Mekelweg 2, 2628 CD Delft

The broaching of a fast rescue craft in following seas.

by

P. de Jong, M.R. Renilson and F. van Walree

Report No. 1896-P

2013

**Proceedings of the 12th International Conference on Fast Sea
Transportation, FAST2013, Amsterdam, The Netherlands.**

FINAL SCIENTIFIC PROGRAM



Monday 2 December

- 9:30 Registration
10:15 **Opening Conference**
10:30 Keynote ir J.L. Gelling Damen Shipyards
11:00 Keynote R. Bogaard KNRM
11:30 *Coffee break*
12:00 Keynote prof. Ir. J. Hopman Delft University of Technology
12:30 Keynote mr. T. Ellis - Specialised Vessel Services
13:00 *Lunch*
14:00 Session 1A New Concepts
P44 Gelling
P06 Orvieto
P32 Shahraki
15:30 *Coffee break*
16:00 Session 2A Seakeeping 2
P35 Olausson
P37 Allen
17:00 **Opening Reception at the Maritime Museum**
- Session 1B Seakeeping 1
P29 Grigoropoulos
P13 Stojanovic
P15 Peterson
- Session 2B Wash
P41 Pinkster
P09 Kuroda

Tuesday 3 December

- 9:30 Session 3A Structural Design 1
P05 Benson
P11 Wu
P45 Misirlis
11:00 *Coffee break*
11:30 Session 4A Structural Design 2
P24 Schiere
P27 den Besten
P12 Tuitman
13:00 *Lunch*
14:00 **Excursions**
- Session 3B Hullform design / Hydrodynamics
P31 Paryshev
P04 Rosenthal
P20 Diez
- Session 4B Seakeeping 3
P26 Walree
P14 Ahmadian
P18 Ommani

Wednesday 4 December

- 9:30 Session 5A Hydrodynamic Loads
P08 Fine
P34 Varyukhin
P38 Serebryakov
11:00 *Coffee break*
11:30 Session 6A Calm Water Resistance
P07 Kinaci
P22 Fossati
P40 Scherer
13:00 *Lunch*
14:00 Session 7A CFD 1
P16 Kobayashi
P17 Tahara
P19 Chen
18:30 **Conference dinner at the Maritime Museum**
- Session 5B Seakeeping 4
P33 Davidson
P48 Tascon
P25 Castro Feliciano
- Session 6B Motion Control 1
P28 Rijkens
P42 Deyzen
P21 Yengejeh
- Session 7B Dynamic Stability
P01 De Jong
P39 Sadat Hosseini
P30 Castiglioni

Thursday 5 December

- 9:30 Session 8A Hydrodynamics
P36 Dogan
P02 Gontsova
P10 Liopoulos
11:00 *Coffee break*
11:30 Session 8A Hydrodynamics
P43 Cleijnsen (Rijkens)
P46 Zangle
12:30 **Conference Closing**
13:00 *Lunch*
- Session 8B Propulsion
P03 Dang
P23 Eslamdoost
P49 Caponetto

This final program is subject to changes

THE BROACHING OF A FAST RESCUE CRAFT IN FOLLOWING SEAS

P. de Jong, Ship Hydromechanics and Structures, Delft University of Technology, The Netherlands

M.R. Renilson, Australian Maritime College, University of Tasmania, Australia, and Higher Colleges of Technology, United Arab Emirates

F. van Walree, Maritime Research Institute Netherlands, The Netherlands

SUMMARY

This paper focuses on investigating the tendency of a fast rescue craft of the Royal Netherlands Sea Rescue Institution (KNRM) to broach in stern and stern-quartering seas by means of quantitative numerical simulation. The aim is to investigate the suitability of a numerical simulation tool, a semi-nonlinear time-domain potential flow boundary element method complemented with additional force components for steering and viscous forces, for this class of problems. The results show that the method can be used to simulate the surf-riding behaviour of this type of vessel, a commonly accepted pre-cursor to broaching behaviour. After inclusion of a limited number of additional manoeuvring coefficients into the method, it was applied to broaching simulations. The results indicate that the method indeed can be applied for predicting the tendency to broach.

NOMENCLATURE

ROMAN

B	Beam	(m)
c	Wave celerity	(m/s)
Fr	Froude number	(-)
GM	Metacentric height	(m)
H	Wave height	(m)
K, N	Manoeuvring moments	(Nm)
L	Length	(m)
LCG	Longitudinal position CG	(m)
r	Yaw rate	(rad/s)
R	Resistance	(N)
S	Wetted surface area	(m ²)
T	Draught	(m)
T	Thrust	(N)
u, v	Surge and sway velocity	(m/s)
U	Forward speed	(m/s)
x, y, z	Spatial reference coordinates	(m)
X, Y, Z	Manoeuvring forces	(N)

NON-DIMENSIONAL PARAMETERS

$$X' = \frac{X}{\frac{1}{2} \cdot \rho \cdot U^2 \cdot B \cdot L}$$

$$Y' = \frac{Y}{\frac{1}{2} \cdot \rho \cdot U^2 \cdot B \cdot L}$$

$$K' = \frac{K}{\frac{1}{2} \cdot \rho \cdot U^2 \cdot B^2 \cdot L}$$

$$N' = \frac{N}{\frac{1}{2} \cdot \rho \cdot U^2 \cdot B \cdot L^2}$$

$$r' = \frac{r \cdot L}{U}$$

$$v' = \frac{v}{U}$$

GREEK

β	Drift angle	(deg)
δ	Water jet nozzle deflection	(deg)
ϕ	Heel angle	(deg)
λ	Wave length	(m)
∇	Volume of displacement	(m ³)
ρ	Density of water	(kg/m ³)
ξ	Long. position in the wave	(m)
ψ	Heel and heading angle	(deg)
ζ	Wave elevation	(m)

SUBSCRIPTS

o	Earth-fixed
a	Amplitude
max	Maximum
mean	Average
tot	Total

An over-dot denotes a derivative with respect to time.

1. INTRODUCTION

Due to their purpose, fast rescue craft can be deployed in extremely rough weather conditions, both offshore and near-shore. The operability and comfortability of these ships can be severely affected by their performance in bow to bow-quartering seas, where large vertical acceleration levels can occur due to frequent wave impacts. Nevertheless, from the viewpoint of safety the performance of these fast small craft in steep stern to stern-quartering seas can be more important.

Under these conditions phenomena including the pure loss of transverse stability, surf-riding, bow diving, and broaching may occur. These phenomena are less researched, both numerically and experimentally, as they require extensive and costly model tests to reliably capture rarely occurring events as broaches, or complex numerical tools, which need to be run for long periods of time. Nevertheless, the IMO Code of Safety for High Speed Craft requires that one demonstrates that the probability of the aforementioned events is acceptably low, or that the consequences are within limits.

Broaching occurs when the wave excited yaw moment exceeds the maximum rudder restoring yaw moment [1]. Typically this can happen when a ship travels in severe following waves and is accelerated to the wave celerity by a wave of the ship length or greater. As a consequence broaching is associated with non-linear asymmetric surging motions and surf-riding followed by large yaw motions and eventually large heeling angles. In extreme cases, the ship can be yawed to an orientation almost parallel to the wave crest causing large heel angles with the risk of considerable damage or even a capsizing [1], [2].

This paper focuses on investigating the tendency of a concept design of a fast rescue craft of the Royal Netherlands Sea Rescue Institution (KNRM) to broach by means of quantitative numerical simulation. The aim is to investigate the suitability of a numerical simulation tool, a semi-nonlinear time-domain potential flow boundary element method complemented with additional force components for steering and viscous forces, for this class of problems. If successful, this would allow a more systematic judgement and comparison of the behaviour in stern to stern-quartering seas of designs of fast seagoing craft, than is possible in free-sailing model tests in a test basin, due to practical reasons as costs and time.

The choice for the KNRM concept design rescue vessel is twofold. First, as part of a large research effort supporting the development of a next generation rescue vessel, the KNRM NH1816, there is a large amount of data available that can be used to support and validate the computations. Second, due to its nature, this type of vessel operates in extreme weather environments at high forward speed in arbitrary wave directions with a specific target location, circumstances that may very well lead to conditions with a high risk of broaching.

The simulation method presented in this paper has already been extensively validated for ship motions at medium to high forward speed in regular and irregular head waves [3], [4], [5]. Moreover, recent work also includes statistic and deterministic validation of motions at high forward speed in stern-quartering waves for a 55 metre patrol vessel [6]. In that study, the comparison between computed and experimental values was carried out statistically, by comparing significant and most probable maximum values, and by comparing time traces directly. For the latter approach, the computation was fed with a reconstruction of the experimental wave elevation. The comparison work showed good agreement between

computed and experimental motions and inspired further investigation into the possibility of the prediction of the onset of broaching presented in the current paper.

To realistically simulate the full extent of a broach and its consequences may be well out of reach of any current state-of-the-art simulation method. A more practical approach is to limit the study to the *onset* of broaching as a measure of the broaching behaviour. Knowing whether a particular vessel has a tendency to broach in a certain wave condition and being able to compare this tendency between alternative designs, particularly where one of the designs already exists, and is known to have acceptable behaviour in following seas, may be sufficient in most cases. The latter approach is followed in the current paper and puts the focus on the initial part of the broach, where nonlinear effects have less effect.

Nonetheless, in order to correctly simulate the tendency to broach requires the simulation method to accurately predict the wave induced forces, manoeuvring forces, steering forces and autopilot behaviour, and the surge balance and subsequent surf-riding behaviour. To make sure these forces are properly included use is made of the results of extensive experiments carried out during the development of the new KNRM NH1816 class rescue craft. These results include calm water trim, sinkage, and resistance, manoeuvring forces obtained with forced oscillation experiments, water jet forces, and free sailing model tests (Figure 1).



Figure 1: Free sailing model tests with KNRM NH1816 Concept 2 in the Seakeeping and Manoeuvring Basin at MARIN

After describing the simulation method and the experiments in more detail in sections 2 and 3, the comparison of the aforementioned experimental data with results obtained from the computational method is presented in section 4. First the running trim, sinkage and calm water resistance are compared, followed by the manoeuvring forces and the steering model. The results show that most of these aspects are captured well, except for the roll-yaw coupling.

Finally the paper concludes with the assessment of the surf-riding behaviour and the tendency to broach of the fast rescue craft by running an extensive set of simulations for broaching and its pre-cursor surf-riding

for a range of forward speeds and regular waves. The outcomes are compared to published results of similar cases and the free running model experiments mentioned previously. It is concluded that the proposed method can indeed be used to study and quantify the broaching behaviour of fast small craft in severe following waves.

2. SIMULATION METHOD

The simulation of broaching in stern to stern-quartering waves is more complicated than simulating ship motions in head to beam seas. This is due to the large amplitude motions occurring not only in the vertical plane but also in the horizontal plane. The forces and moments are dependent on the longitudinal position of the vessel in the wave in a non-linear manner, requiring a full time domain simulation. This is unlike the behaviour in head seas, where for a large extent it is enough to consider the average position of the vessel in the wave. In addition to being capable of dealing with large motions in six degrees of freedom, also to predict broaching behaviour it is necessary to include adequate modelling of steering capabilities and propulsion into the simulation method.

As the steepness of the waves increases, so does the tendency to broach, requiring simulation methods to deal with non-linear effects both in the waves and in the body motions. The resulting large variations in the instantaneous submerged body have an influence on the hydrostatic forces, the wave exciting forces, and the hydrodynamic disturbance forces. In extreme cases the large relative motions may lead to deck immersion, requiring incorporation of the dynamics of water on deck. Similarly, wind loads on the emerged part of the geometry may have an important influence on motion damping and roll excitation and may have a significant influence on the severity of extreme roll motions.

Another feature of the behaviour of vessels at forward speed in following waves is the low encounter frequency. This low encounter frequency has inspired some authors to deal with surf-riding and broaching problems in a quasi-steady fashion, see for instance [1]. As a result of these low encounter frequencies potential flow damping is only slight and viscous forces due to friction and flow separation are important.

To completely deal with the above requires a fully non-linear simulation method, preferably including viscous flow effects. Up to now, these methods require a prohibiting amount of computational time and effort for a full time domain simulation, and until now are mostly used to derive manoeuvring coefficients for use in more generic programs to simulate manoeuvring performance.

Here a time domain panel method is used, employing a linearization of part of the hydrodynamic problem combined with semi-empirical viscous models to enable faster computations and enabling full time domain simulation. This method, termed PANSHIP, is described in detail in [3] and [5], and can be characterized by:

- Three-dimensional transient Green function to account for linearized free surface effects, exact forward speed

effects, mean wetted surface, mean radiated and diffracted wave components along the hull and a Kutta condition at the stern;

- Three-dimensional panel method to account for Froude-Krylov forces on the instantaneous submerged body;
- Cross flow drag method for viscosity effects;
- Resistance obtained from pressure integration at each time step combined with empirical viscous drag;
- Propulsion using propeller open water characteristics or a semi-empirical water jet model;
- Motion control and steering using semi-empirical lifting-surface characteristics, water jet steering, and propeller-rudder interaction coefficients;
- Empirical viscous roll damping;
- Autopilot steering;

3. EXPERIMENTS

As part of the development of a new generation of rescue vessel, the NH1816, for the Royal Netherlands Sea Rescue Institution (KNRM), a design group, formed by the Delft University of Technology, W. de Vries Lentsch (the designers of the existing boats), and the High Speed Craft Department of Damen Shipyards, created two design alternatives. Concept 1 was a modest adaptation to the existing 'Arie Visser' class life boat, Concept 2 was a new design based on the AXE Bow concept. The emphasis was for both designs on improving both the operability and the habitability.

In order to judge the relative merits of both designs, extensive model tests were carried out at MARIN and at Delft University with both design concepts and the existing 'Arie Visser' class life boat. The latter served as a benchmark design. Keuning *et al.* [7] reported on these tests and their outcomes. The main result was the selection of Concept 2 to serve as basis for the final design for the new generation of KNRM life boats.

The experiments included resistance and running trim and sinkage in calm water, the behaviour in head seas at high forward seas in towing tank No. 1 of Delft University (measuring 145 m long, 4.25 m wide, and 2.5 m deep) and free sailing model tests in stern quartering and following seas in the Seakeeping and Manoeuvring Basin of MARIN (measuring 225 m long, 50 m wide, and 5 m deep). For the free sailing tests the models were fitted with a twin water jet arrangement with steering buckets, controlled by an autopilot. With the benchmark design and Concept 2 a series of captive manoeuvring experiments with a model fitted under a hydraulic actuated oscillator was carried out at Delft University at a later stage in the design process.

Due to the large amount of data that became available during these experiments Concept 2 was chosen for the current study. A lines plan of this design is given in Figure 2, together with the main particulars in Table 1: Main particulars of KNRM Concept 2. For this particular

study use was made of the calm water resistance and running trim and sinkage and the results of the captive manoeuvring tests.

Table 1: Main particulars of KNRM Concept 2

Description	Symbol	Unit	Value
Length over all	L_{oa}	m	21.00
Length between perp.	L_{pp}	m	18.50
Beam over all	B_{oa}	m	6.35
Draught	T	m	1.17
Displacement	∇	tonnes	39.9
Long. Pos. CG w.r.t. app	LCG	m	6.89
Wetted surface	S	m ²	78.60
Metacentre height	GM	m	1.46

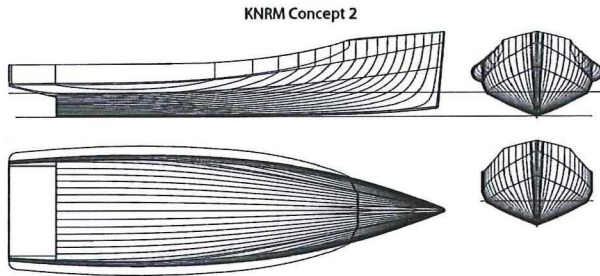


Figure 2: Lines plan of KNRM Concept 2

For the captive manoeuvring experiments a 1:10 scale model was mounted under a 6 degrees-of-freedom hydraulic oscillator in the towing tank No. 1 of Delft University, as shown in Figure 3. To simplify the model, it was constructed from solid high density polyurethane without the pronounced tube. The model was connected to the oscillator by means of a decoupled system comprising two force transducers capable of measuring forces and moments in all 6 degrees of freedom.



Figure 3: Model Concept 2 mounted under 6 DOF oscillator

The tests that were performed included steady drift tests and forced sway and yaw oscillations. The forced sway and yaw oscillations were performed at a range of frequencies from 0.126 to 0.505 rad/s and amplitudes of 0.750 m and 2.25 deg at a forward speed of 25 kts (full scale values).

A steady drift angle was tested up to 10 deg at a forward speed of 25 kts and 35 kts full scale. These tests have been performed at a number of different steady orientations, with different combinations of trim, heel, and rise, to simulate the influence of the position of the vessel in the wave on the manoeuvring coefficients. In order to investigate the influence of skegs, the steady drift tests were carried out for the model with and without skegs. For the purpose of the current paper the scope is limited to the results for Concept 2 without skegs and tube.

Uncertainty analysis has been performed on the results of these experiments and the resulting uncertainty bounds are reported by the error bars in the figures below, where available.

4. MODEL VALIDATION AND ADJUSTMENT

The results of the model experiments described in the previous section were used to validate the outcomes of the computational method and in some cases were used to fine tune the method in order to better reflect the hydrodynamic characteristics of the design under consideration. When reporting forces and moments the reference system depicted in Figure 4 was used. The origin of the system is located in the centre of gravity.

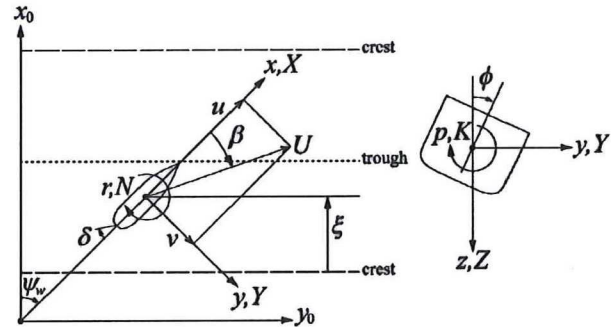


Figure 4: Axis system used for the manoeuvring forces

Both surf-riding and broaching require fully free sailing simulations that accurately capture the surge behaviour. In order to verify whether the model captures this behaviour, the predicted calm water trim, sinkage, and resistance using the numerical model were compared with the experimental outcomes.

To determine the calm water running attitude and total resistance, the semi-nonlinear simulation method was run iteratively for each forward speed until the linear underwater panel geometry matched the orientation of the vessel at the end of an iteration within a certain range. The resistance included skin friction according to the ITTC'57 friction line and a form factor $1+k$ of 1 was applied. The transom was assumed to be ventilated and the pressure drop towards the ventilated transom was modelled by an empirical correction as published by Garme [8].

Figure 5 shows a comparison of the predicted total resistance compared to the measured value (scaled to full scale). Although the absolute value is under-predicted,

the overall behaviour and slope is captured well in the computations. The latter is necessary for modelling the surge behaviour.

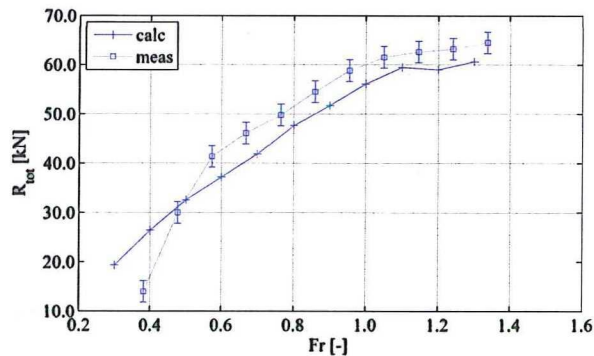


Figure 5: Total calm water resistance

In the simulation method a semi-empirical water jet model has been incorporated, that was used for the free sailing simulations for surf-riding and broaching. The water jet model and its empirical coefficients were developed at MARIN by using their extensive data on water jet powered vessels. In this model, first the gross thrust of the water jet is determined by the momentum balance of the water jet. Subsequently, the thrust and the steering force at the deflected nozzle of the water jet are computed by applying conservation of momentum to the thrust deflection. The computation is supported by a number of empirical coefficients.

Figure 6 shows a comparison of the predicted and measured water jet forces and steering moment on a typical high speed vessel obtained from MARIN [9]. Although the degrading of the thrust force for increasing bucket deflection angle is under-predicted, the generated side force and steering moment are well-predicted.

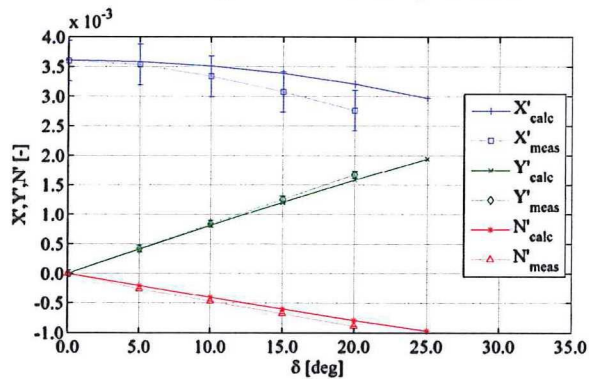


Figure 6: Water jet steering model, example of agreement with experimental data, $Fr = 0.37$

The procedure to obtain the water jet rpm was to match the thrust generated by the water jets with the calm water resistance predicted by the simulation method for a forward speed at the predicted running attitude in calm water. The next step was to compare the manoeuvring forces predicted by the simulation method with the experimental values. Although the predictions of the sign and magnitude of the sway, yaw, and roll were in reasonable agreement with the experiments for constant

drift angle tests, it was decided to correct the differences by adding experimentally obtained manoeuvring coefficients into the simulation method. Figure 7 shows the measured, calculated, and corrected calculated non-dimensional side force for tests at a constant drift angle at a Froude number of 0.96, including the uncertainty bounds for the experiments.

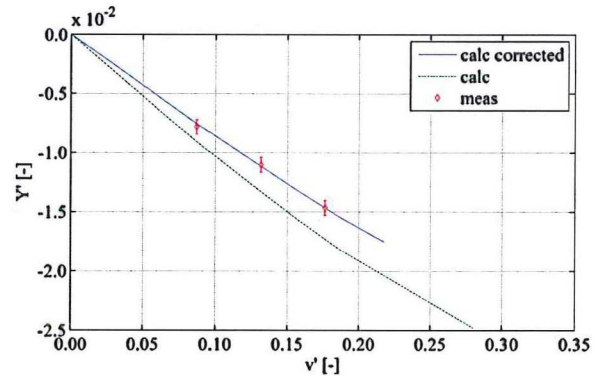


Figure 7: Correction of the predicted side force

Figure 8 shows the resulting comparison of calculated and measured sway, yaw, and roll forces for a constant drift angle. The non-dimensional forces are plotted as functions of the non-dimensional sway velocity.

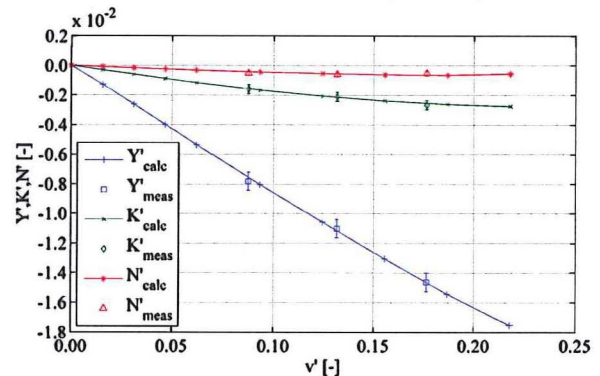


Figure 8: Calculated and measured forces for constant drift angle tests

Next, a comparison was undertaken of the measured and calculated sway and yaw forces for forced oscillations in sway and in yaw. As an example Figure 9 shows the non-dimensional force amplitudes for oscillations in yaw.

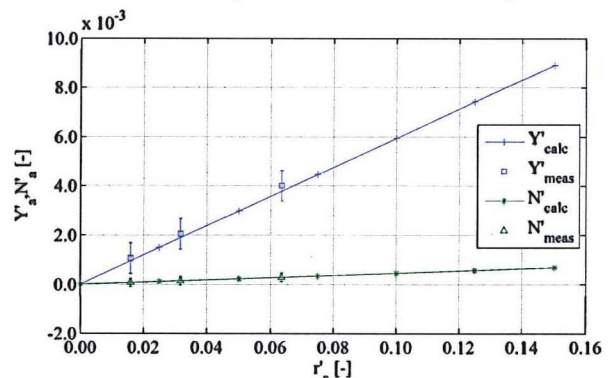


Figure 9: Calculated and measured sway and yaw force amplitudes for forced oscillation tests in yaw

During the calculations the same manoeuvring coefficients implemented during the constant drift computations were used. The results show that the coefficient values that worked well for the steady tests also worked well for the forced oscillations. New coefficients were implemented for the coupling between sway and yaw and vice versa. The sway force amplitude for forced oscillations in yaw was found to be under-predicted.

After the addition of the correcting manoeuvring coefficients, it was found that the simulation method was accurately capturing the manoeuvring characteristics of the KNRM Concept 2.

A final validation was made by investigating the coupling between heel and yaw that may be of significant influence on a broach [10]. Most literature [10] shows that typically when heeled to starboard, a vessel at forward speed experiences a turning moment to port. Nevertheless, the opposite is also found in some cases. Unpublished data from PMM tests with a high speed craft carried out at MARIN show for high Froude numbers a starboard turning moment when heeled to starboard. As shown by the solid lines in Figure 10, the simulation method predicted a starboard turning moment. Unfortunately for this particular craft no experimental data is available for the roll yaw coupling.

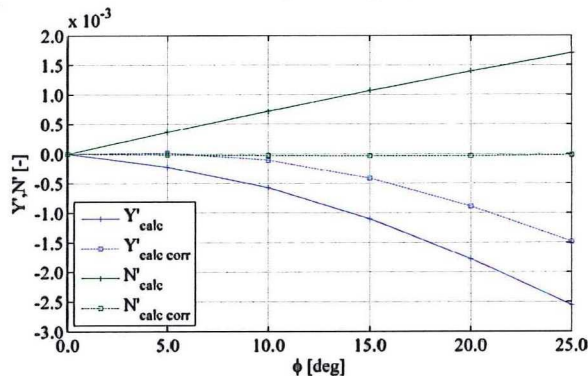


Figure 10: Computed sway force and yaw moment dependence on heel angle (Fr = 0.50)

In the current method the orientation of the vessel in the water is accounted for by adjusting the incoming flow velocity at each panel. Nonetheless, the panels remain on the (upright) mean wetted surface – even when heeling – due to the linear approach. Hence, the heel angle is not picked up by the hydrodynamic solution directly, but only indirectly by the changed inflow velocities at each panel originally submerged panel, possibly causing the inaccurate prediction of the forces under heel.

A possible solution could be to perform a series of steady captured numerical simulations with the panels distributed over the heeled wetted surface, and implementing the results into a coefficient that is used for the free sailing simulations.

For the purpose of this paper it was decided to remedy this by suppressing the sway force and yaw moment due to a heel angle altogether. This was done by again injecting additional linearized manoeuvring coefficients

in the equations of motion solved by the simulation method. The dashed lines in Figure 10 show that until heeling angles of 10 degrees the forces are effectively suppressed. As only the onset of a broach is investigated in the paper, it was expected that the influence of heel on the results would be limited. Comparison of broaching simulations with and without this suppression confirmed this.

5. RESULTS

After validating the different components of the simulation method and implementation of additional force components to better represent the manoeuvring characteristics of the vessel, the current section focuses on the outcomes of free sailing simulations in following waves. First, the behaviour in pure following waves (with a heading angle of 0 degrees) was studied in terms of the tendency to surf-ride. Second, the initial heading angle was set to 20 degrees to study the tendency to broach.

5.1 SURF-RIDING

To investigate the tendency to surf-ride an extensive series of simulations in following regular waves was carried out. The parameters that were varied during the runs are presented in Table 2. Each simulation consisted of a free sailing test of 100 seconds real time in a particular regular wave with a constant water jet rpm set according to the calm water resistance at the given Froude number.

This resulted in a minimum of 5 wave encounters and an average of 11 wave encounters in cases where the vessel was not surf-riding. Naturally, in cases when the vessel did surf the number of wave encounters was less. In those cases 100 seconds real time was sufficient to let the vessel settle in a steady state. The time step was set in such way that the vessel travelled one typical panel size per time step. Typically, results of the computations converged when the panel model of the vessel had 60 panels over the length.

At the start of the run the incoming wave (with its crest at the CG of the vessel), as well as the computed accelerations, were ramped up in 25 time steps. During this period the vessel travelled about 40% of the ship length. After that the vessel was completely free sailing. Time traces of the rigid body motions, velocities, and accelerations, amongst others, were saved for each run and analysed.

Table 2: Parameter ranges investigated

Description	Parameter	Ranges
Forward speed	Fr	0.20 – 0.60
Wave steepness	H/λ	0.03 – 0.12
Wave length	λ/L	1.0 – 2.0

Next, the time traces were analysed for the tendency to surf-ride. The definition of surf-riding is that was used here is given in Table 3. Typically, surf-riding is defined

as the situation when a vessel, which is initially traveling slower than the waves overtaking it, is accelerated to the wave celerity after which the forward speed of the vessel, and its longitudinal position in the wave, remains constant. The vessel is ‘captured’ by the wave, usually on the front face of the crest that was initially overtaking the vessel. A marginal surf is defined as the situation in which the vessel is accelerated to 90 per cent of the wave celerity or over, but does not reach the wave celerity itself, *i.e.* the waves are still slowly over taking the vessel. Marginal surf-riding can generally be characterised by strong asymmetrical surge motions, where the vessel spends relatively more time close to the wave celerity in each cycle, and hence spends a lot more time in one longitudinal region of the wave (usually the wave face), compared to other regions (usually the back of the wave).

Table 3: Definition of surf-riding

Description	Surf-riding	Marginal surf-riding
Forward speed	$U = c$	$U \geq 0.9 \cdot c$

The opposite situation as described above can also occur: initially the vessel is traveling faster than the incident waves but after passing through the wave trough does not manage to ‘climb’ over the crest following the trough and remains captured on the back face of this crest. Technically one cannot speak of surf-riding in this case, but rather the term ‘wave blocking’ introduced by Maki *et al.* [11] seems more appropriate.

Figure 11 presents an overview of surf-riding in terms of the initial velocity and the length of the incident waves for a constant wave steepness of 0.06 by representing the outcome (surf-riding; marginal surf-riding; no surf-riding) of each simulation by a symbol. The figure includes a line at which the initial velocity equals the wave celerity. Above this line, the vessel is not surf-riding, but rather is being blocked by the wave as discussed above. In the top left corner a region is visible in which the vessel does manage to overtake the wave.

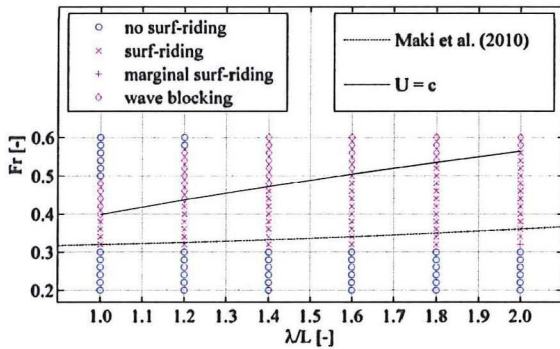


Figure 11: Surf-riding behaviour as a function of wave length and Froude number for $H/\lambda = 0.06$

The line marked ‘Maki’ marks a surf-riding boundary as was found by Maki *et al.* [12] for the ONR tumblehome

ship and is included for reference. The results obtained in the current study and these from Maki show a very similar surf-riding boundary for $\lambda/L = 1.0$ while for $\lambda/L = 2.0$ the Maki limit tends to somewhat higher Froude numbers.

Figure 12 presents a similar overview for a constant wave length to ship length ratio of 1.20. The line marked ‘Maki’ and ‘Thomas’ mark surf-riding boundaries as published by Maki *et al.* [12] as mentioned before and by Thomas and Renilson [13] for a fishing trawler, again for reference purposes. The surf-riding boundaries from the current study and the reference boundaries are again quite similar.

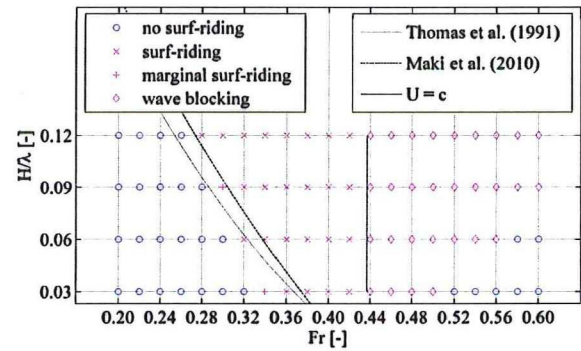


Figure 12: Surf-riding behaviour as a function of Froude number and wave steepness for $\lambda/L = 1.20$

Finally, in order to confirm whether the simulations showed a reasonable and smooth behaviour, plots were made of the percentage of the difference between the mean velocity during the simulations and the wave celerity in Figure 13 and the calm water speed in Figure 14.

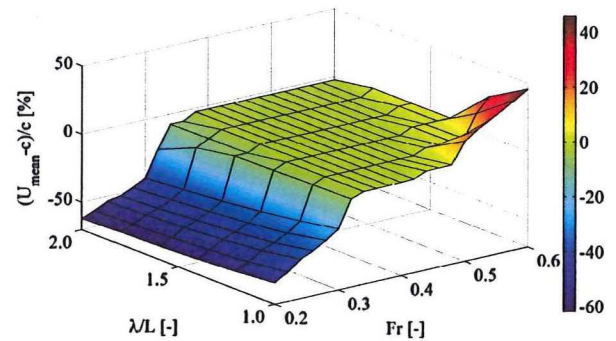


Figure 13: Percentage difference mean velocity and wave celerity

Three regions can be distinguished:

- The region of overtaking waves is apparent for the lower Froude numbers: the mean forward speed is lower than the wave celerity and nearly equal to the calm water forward speed. This region is followed by a sharp increase in the mean velocity marking the surf-riding boundary.

- In the surf-riding region the difference between the mean forward speed and the wave celerity is zero. When the mean forward speed drops below the calm water forward speed, the vessel experiences a transition from surf-riding to wave blocking.
- Wave overtaking is indicated by the increase in velocity on the far right of Figure 13, and marks the region of ‘no surf-riding’ visible in the top left of Figure 11. Figure 14 shows that although the mean forward speed recovers somewhat in this phase, it remains below the calm water forward speed.

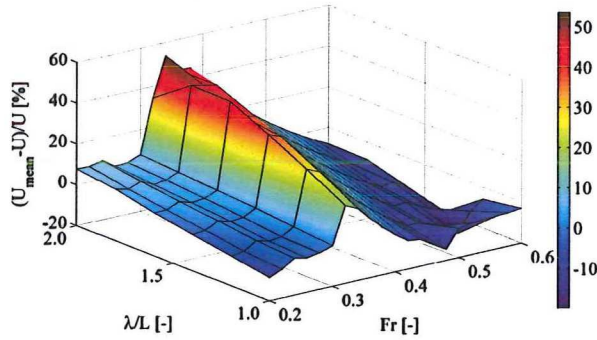


Figure 14: Percentage difference mean velocity and calm water velocity

5.2 BROACHING

The broaching behaviour was studied in the same manner as the tendency to surf-ride. Again free sailing simulations of 100 seconds each were carried out for the same range of conditions and forward speeds, but the initial heading angle to the waves was set to 20 degrees with the auto-pilot activated to attempt to keep this heading. The control algorithm for the nozzle angles was as follows:

$$\delta = b_{\delta\psi} \cdot \dot{\psi} + c_{\delta\psi} \cdot \psi \quad [1]$$

In this equation ψ is the deviation of the desired heading, and δ the water jet nozzle deflection angle. The coefficients of the auto-pilot and the limits to the deflection angle are presented in Table 4.

Table 4: Auto-pilot settings for course keeping

Description	Symbol	Unit	Value
Damping coefficient	$b_{\delta\psi}$	deg/(deg/s)	9.49
Proportional coefficient	$c_{\delta\psi}$	deg/deg	3.00
Max deflection angle	δ_{\max}	deg	23
Max deflection speed	$\dot{\delta}_{\max}$	deg/s	10

To analyse the tendency to broach, broaching and marginal broaching were defined as presented in Table 5. These definitions are similar to the ones published by Renilson and Tuite [14]. These definitions were developed by Renilson and Tuite based on extensive analysis of their broaching simulations.

Figure 15 and Figure 16 show the overview of the broaching behaviour in a similar manner as previously was done for surf-riding. Included are: a dotted line representing the situation that the initial ship speed matches the wave celerity; and contour lines that indicate the maximum course deviation during each simulation. The overall behaviour shows similar features as in other studies, refer to for example [2].

Table 5: Definition of broaching

Description	Broach	Marginal broach
Heading deviation	$\psi \geq 20^\circ$	$\psi \geq 20^\circ$
Rudder angle	$\delta = \delta_{\max}$	$\delta = \delta_{\max}$
Yaw rate	$r > 0$	$r > 0$
Yaw acceleration	$\dot{r} > 0$	-

Figure 15 does indeed show that broaching and surf-riding are closely linked phenomena. The vessel only experiences broaching when it is at least surf-riding. Only then is the vessel long enough in a longitudinal position in the wave to experience enough wave induced upsetting yawing moment. Also clearly visible is that the upper boundary of broaching runs parallel to and remains well below the forward speed equals wave celerity limit for the wave steepness $H/\lambda = 0.06$. For this wave steepness only in two cases a full broach was predicted according the definition given in Table 5. Nevertheless, studying the time traces, the yaw acceleration often displayed small fluctuations around zero near the time of broaching, explaining the seemingly arbitrary distinction between marginal and full broaches for the lower values of the wave steepness.

Figure 16 shows the dependency of the predicted broaching behaviour to the wave steepness for a wave length of $\lambda L = 1.20$. As can be expected, the tendency to broach increases with greater wave steepness. Both figures show that the largest tendency to broach occurs at a calm water forward speed just exceeding the surf-riding boundary, and still below the wave speed. This region is indicated by the largest yaw excursions being found near the surf-riding boundary. This is caused by two different mechanisms.

First, the longitudinal equilibrium position shifts forward in the wave with increasing thrust in the same wave, resulting in a lower wave upsetting moment as the stern moves away from the wave crest and therefore less tendency to broach. Second, as the vessel is travelling faster while surf-riding than it would with the same rpm setting in calm water, it experiences a reduction in thrust force relative to the wave speed it travels at and therefore in maximum steering moment. Also this effect diminishes with increasing rpm setting. Despite that, it should not be recommended to increase the thrust to avoid broaching. There is always a risk on a longer, and therefore faster, wave that will cause broaching if the vessel travels faster, even if at the original slower vessel speed this wave would not even cause surf-riding.

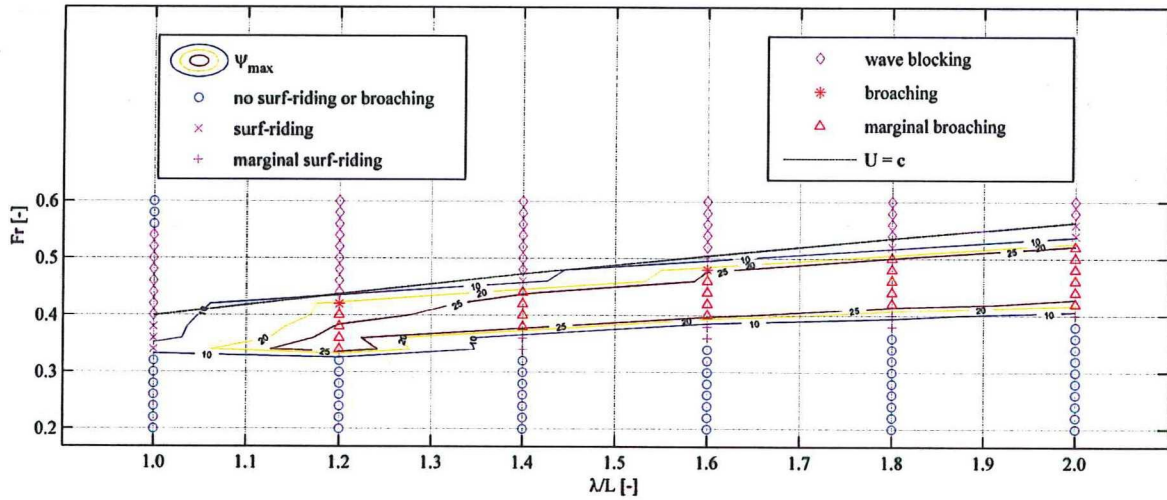


Figure 15: Broaching as a function of wave length and Froude number for $H/\lambda = 0.06$

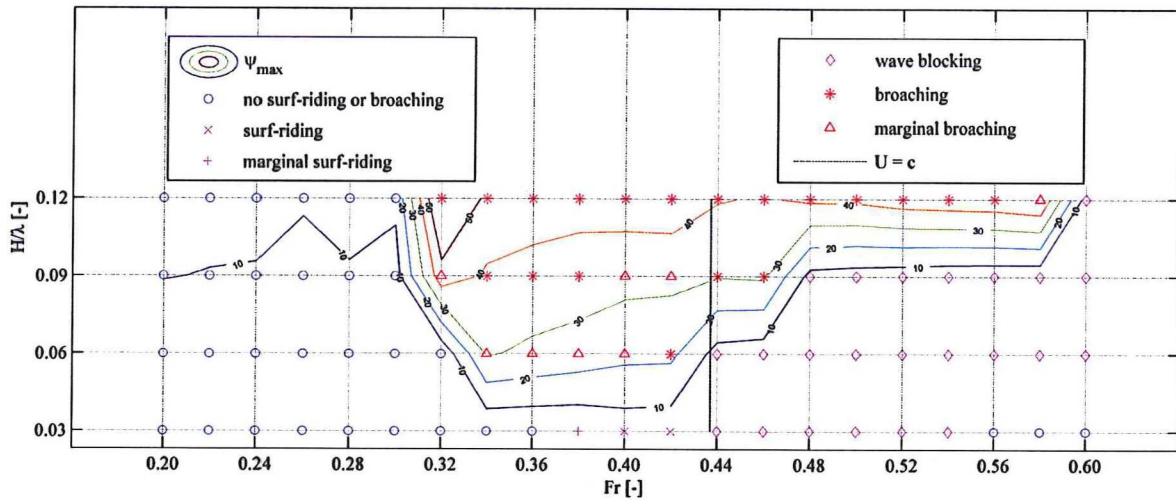


Figure 16: Broaching as a function of Froude number and wave steepness for $\lambda/L = 1.20$

Figure 17 presents X_{wave} , the longitudinal force from the wave, and $-\Delta X$, the (negative) resultant of the thrust minus the calm water resistance force in the wave compared to calm water as functions of the longitudinal position in the wave. Figure 18 presents the same for the wave upsetting yaw moment N_{wave} and the (negative) maximum steering moment $-N_{\text{steer}}$. The particular case shown ($Fr = 0.46$, $H/\lambda = 0.06$, $\lambda/L = 1.60$) reflects a case in which a broach was observed. The analysis has been performed for two heading angles, 20 degrees and 40 degrees, being the initial heading angle and the heading angle associated with the broach.

The figure has been obtained by performing a series of quasi-steady simulations where the vessel was kept in a constant longitudinal position relative to the wave, while travelling at the wave speed. During each simulation the vessel was free to heave, pitch, and roll. In order to obtain the forces mentioned above (defined in accordance with Figure 4), the process was performed twice. Once without water jet for the wave force and moment and once with the water jet activated with a

maximum nozzle deflection to generate a steering moment to counter the wave upsetting moment. Where the (delta) resistance crosses the longitudinal wave force the vessel is in a stable longitudinal equilibrium.

For the heading angle of 20 degrees (the blue lines in Figure 17 and Figure 18) the vessel is in a stable longitudinal equilibrium at $\xi/\lambda = 0.43$. At that same instance the maximum steering moment is only slightly larger than the upsetting yawing moment due to the wave. As a broach was predicted in this case, one may have expected that the steering moment was exceeded by the upsetting moment in the quasi-steady analysis. The fact that this did not happen, may be related to a number of factors, amongst which:

- The actual heading angle at the broach is different to the initial angle of incidence of 20 degrees, leading to a larger wave induced yaw moment;
- The dynamics, ignored by the quasi-steady approach, may have sufficient influence on the moments;

- The time it takes the water jet to reach its maximum nozzle angle in the dynamic situation is not accounted for in the quasi steady simulations.

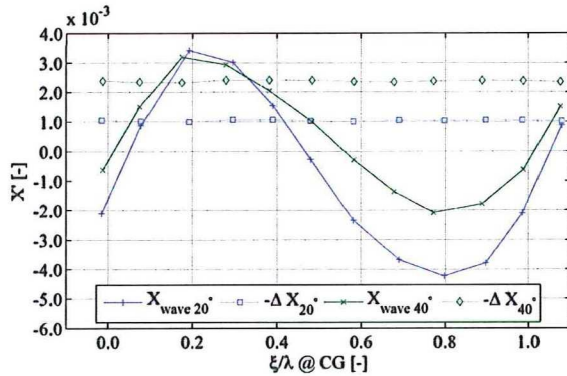


Figure 17: Longitudinal wave force and resistance as functions of the non-dimensional position in the wave for $\psi_w = 20^\circ$ (blue) and $\psi_w = 40^\circ$ (green)

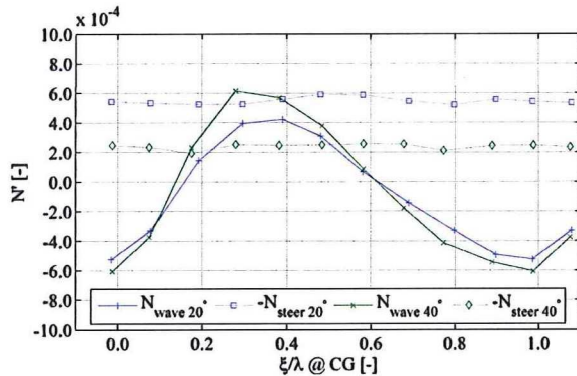


Figure 18: Wave upsetting moment and steering moment as functions of the non-dimensional position in the wave for $\psi_w = 20^\circ$ (blue) and $\psi_w = 40^\circ$ (green)

The first factor mentioned above can be confirmed by studying the information presented for the heading angle of 40 degrees (the green lines in the figures). The thrust decreased for this heading angle (at the same rpm setting as before), leading to an altered longitudinal equilibrium position in the wave at $\xi/\lambda = 0.35$. The wave upsetting moment has increased, whereas due to the reduced thrust also the steering moment is reduced. In fact, for the 40 degree heading angle the upsetting moment exceeds the maximum steering moment, confirming the first point mentioned above.

The reduction of the water jet forces is caused by the craft surf-riding on a wave, leading to a higher forward speed of the craft and a higher inflow velocity into the water jet compared to calm water. This in turn leads to a lower thrust force generated by the water jet compared to the calm water. This effect increases for increasing heading angle, as the component of the forward speed in the wave direction needs to stay equal to the wave celerity when surf-riding.

From this discussion it may be concluded that although quasi-static analysis of the dependency of the forces on the longitudinal position in the wave may give a good indication of the tendency to broach, a number of factors

may be overlooked by applying the simplified quasi-steady approach used here. To get a complete picture of a broach, the quasi-steady analysis may need to be performed for a range of heading angles.

6. CONCLUDING REMARKS

The paper describes an investigation into the tendency to broach of a fast rescue craft of the Royal Netherlands Sea Rescue Institution (KNRM) by means of numerical simulation. The aim of the investigation was to determine the suitability of a numerical simulation tool, a semi-nonlinear panel method with additional force contributions, for this class of problems. The craft that was used in this research was a concept design for a fast rescue boat based on the AXE Bow concept, that has been extensively studied experimentally.

The time domain panel method that was used employed a linearization of the hydrodynamic potential flow problem on the mean wetted surface and on the free surface. The method included exact forward speed effects and computed the hydrostatic and Froude-Krylov forces on the instantaneous wetted surface. Viscous effects were accounted for by semi-empirical formulations. Water jet propulsion and steering and an auto pilot were included.

In order to validate the numerical model, first computed values of the calm water trim, sinkage, and resistance and the steady and oscillating horizontal plane manoeuvring forces were compared with experimental results. The steady calm water results compared well. Although trends were captured well for the manoeuvring forces, a number of extra manoeuvring coefficients were introduced in the simulation method making it possible to more accurately capture the steady and unsteady manoeuvring forces. No experimental roll yaw coupling results were available for the particular craft studied. Nevertheless, the roll yaw coupling showed an opposite sign than usually can be expected and for that reason was suppressed in the simulation method for the results presented in the paper. This was considered adequate to predict the onset of a broach, although it is clearly not appropriate if the full trajectory of the broach is required.

Finally the method was applied to the surf-riding behaviour and the tendency to broach of the rescue craft. Surf-riding is generally seen as a pre-cursor to broaching and was shown to be captured well by the simulation method. Three dimensional plots of the mean forward speed showed that as the initial forward speed increased (by increasing the water jet rpm) the craft transitioned smoothly from regular surging to asymmetric surging (known as marginally surf-riding), to full surf-riding, and finally to wave over-taking. The results for surf-riding for the rescue craft showed the same trends as surf-riding results obtained by other authors for other vessels.

The results for broaching showed the method was able to predict the tendency to broach. Overview plots of the broaching region, with contour lines indicating the maximum yaw excursion, showed expected behaviour. The largest yaw excursions were occurring near the

lower initial velocity bound of the broaching region – where the steering moment is relatively low due to the lower rpm settings. The overall features of the broaching region were comparable to what can be found in literature.

For one case where the craft broached, additional quasi-steady analysis was carried out to compare the outcomes of the quasi-steady approach with the full dynamical simulations and to study the broaching behaviour in more detail. The results showed that the simple quasi-steady approach missed some of the dynamics of the broaching, related to the changing angle of incidence in the wave and the dynamics of the water jet steering, and therefore may be under-predicting the tendency to broach. However, a more sophisticated quasi-steady approach may help to understand the physics of what is occurring when a vessel broaches, and may even be of use to predict the likelihood of broaching in the future. This needs to be investigated further.

Future work includes investigating whether a more sophisticated model of the flow separating from the transom leads to better prediction of the manoeuvring forces and further investigation of the roll-yaw coupling.

Application of the method on different design concepts and on the influence of design details as skegs and the tube around the KNRM craft may shed more light on the ability of the proposed method to distinguish the tendency to broach of different designs.

REFERENCES

1. Renilson, M.R. and Driscoll, A., 'Broaching – An investigation into the loss of directional stability in severe following seas', *Transactions Royal Institution of Naval Architects*, Vol. 124, pp. 253-273, 1982.
2. Renilson, M.R., 'An investigation into the factors affecting the likelihood of broaching-to in following seas', *Proceedings of the 2nd International Conference on Stability of Ships and Ocean Vehicles*, pp. 551-564, Tokyo, Japan, 1982.
3. Walree, F. van, 'Development, Validation and Application of a Time Domain seakeeping method for High Speed Craft with a Ride Control System', *Proceedings of the 24th Symposium on Naval Hydrodynamics*, pp. 475-490, Fukuoka, Japan, 2002.
4. Jong, P. de and Walree, F. van, 'The Development and Validation of a Time Domain Panel Method for the Seakeeping of High Speed Ships', *Proceedings of the 10th International Conference of Fast Sea Transportation*, pp. 141-154, Athens, Greece, 2009.
5. Jong, P. de, *Seakeeping behavior of high speed ships - An experimental and numerical study*, PhD thesis, Delft University of Technology, 2011.
6. Walree, F. van and Jong, P. de, 'Validation of a time domain panel code for high speed craft operating in stern quartering seas', *Proceedings of the 11th International Conference of Fast Sea Transportation*, pp. 209-216, Honolulu, USA, 2011.
7. Keuning, J.A., Visch, G.L., Gelling, J.L., Vriesch Lentsch, W. de, and Burema, G., 'Development of a new SAR boat for the Royal Netherlands Sea Rescue Institution', *Proceedings of the 11th International Conference of High Speed Sea Transportation*, pp. 797-806, Honolulu, USA, 2011.
8. Garne, K., 'Improved time-domain simulation of planing hulls in waves by correction of the near-transom lift', *International Shipbuilding Progress*, Vol. 52, No. 3, pp. 201-230, 2005.
9. Walree F. van, Quadvlieg, F.H.H.A., and Jurgens, A.J., *Captive tests on a AMD2400 high speed ferry*, MARIN Report 16794-2-DTM, 2001.
10. Renilson, M.R. and Manwarring, T., 'An investigation into roll/yaw coupling and its effect on vessel motions in following and quartering seas', *Proceedings of the 7th International Conference on Stability of Ships and Ocean Vehicles*, pp. 452-459, 2000.
11. Maki, A., Umeda, N., Renilson, M.R., and Ueta, T., 'Analytical methods to predict the surf-riding threshold and the wave-blocking threshold', *To be published in: Journal of Marine Science and Technology*, 2013.
12. Maki, A., Umeda, N., Renilson, M.R., and Ueta, T., 'Analytical formulae for predicting the surf-riding threshold for a ship in following seas', *Journal of Marine Science and Technology*, Vol. 15, pp. 218-229, 2010.
13. Thomas, G.A. and Renilson, M.R., 'Surf-riding and loss of control of fishing vessels in severe following seas', *Transactions of the Royal Institution of Naval Architects*, pp. 21-29, 1991.
14. Renilson, M.R. and Tuite, A.J., 'Broaching-to – A proposed definition and analysis method', *Proceedings of the 25th American Towing Tank Conference*, Iowa, USA, 1998.

ACKNOWLEDGEMENT

The authors would like to express their appreciation to the Royal Netherlands Sea Rescue Institution (KNRM), W. de Vries Lentsch Yacht Designers and Naval Architects, and the High Speed Craft Department of Damen Shipyards for their kind permission to use the experimental data and the particulars and lines plan of the KNRM 1816 rescue craft design project.

